Journal of Thermal Analysis and Calorimetry (2019) 137:1249–1254
https://doi.org/10.1007/s10973-019-08030-0

Thermal properties of electrospun polyvinylpyrrolidone/titanium tetraisopropoxide composite nanofibers

Orsolya Kéri[1] · Péter Bárdos[1] · Stefan Boyadjiev[1,3] · Tamás Igricz[2] · Zsombor Kristóf Nagy[2] · Imre Miklós Szilágyi[1]

Received: 4 December 2018 / Accepted: 17 January 2019 / Published online: 12 February 2019

Abstract
In this work, polyvinylpyrrolidone/titanium tetraisopropoxide (PVP/TTIP) composite nanofibers were prepared by electrospinning from alcoholic solutions. The morphology and the properties of the fibers were investigated by SEM, Raman spectroscopy, and XRD. The thermal properties and the evolved gases were studied in detail by TG/DTA-MS. The as-spun 800–900-nm-thick PVP/TTIP fibers were then, respectively, annealed in different atmospheres (air and nitrogen) and at different temperatures (550 °C, 900 °C) in order to obtain anatase and rutile TiO_2 nanofibers. The investigation of the thermal properties was important before the preparation of the oxide nanofibers, because based on them the crystallinity and the composition of the TiO_2 nanofibers could be controlled. Metal oxide nanofibers with a slightly smaller diameter, made up mostly by anatase TiO_2, were successfully prepared when the annealing was done at 550 °C, while at 900 °C, rutile TiO_2 fibers were obtained. If nitrogen atmosphere was applied, the nanofibers contained some carbon residue as well.

Keywords TG/DTA-MS · Polyvinylpyrrolidone · Titanium tetraisopropoxide · TiO_2 · Nanofiber · Electrospinning

Introduction

The preparation of nanocomposites with well-controllable morphology and properties nowadays is a really important task [1, 2]. Many different methods exist for synthesizing various composites, one of them is electrospinning [3–6], by which technique uniform nanofibers can be produced with high specific surface area. Although it has a simple setup, the reproducibility is exceptional and the properties (e.g., diameter, specific surface area, composition) of the product can be controlled precisely. During the process, high voltage is applied to a polymer solution or melt, which can also contain the precursor salt of metal oxides. Due to the electric field, charged jets erupt from the surface of the liquid, which stretch to ultrathin continuous fibers and dry mid-flight before reaching the grounded collector. The use of electrospinning allows the production of nanomaterials with diverse properties; thus, there is a wide variety of applications for them. There are examples when the electrospun nanofibers were applied in air filtration [7], photocatalysis [8, 9], gas sensing [10, 11], thermal energy storage [12], optical sensors [13], or for encapsulating biomaterials [14], etc.

Numerous metal oxide nanofibers (e.g., ZnO, TiO_2, MnO_2, WO_3, V_2O_5, NiO, SnO_2, Fe_2O_3) [15] or composites (e.g., NiO/ZnO [16], SnO_2/TiO_2 [17], carbon/MnO_2 [18]) containing different metal oxides can be easily prepared by electrospinning. Out of these oxides, TiO_2 nanofibers are the most widely researched. They can be used in gas sensing [19], photocatalysis [20], solar cells [21], electrochemical biosensing [22], etc. For the preparation of TiO_2, many precursors are available, e.g., titanium tetrabutoxide, titanium chloride, titanium tetraisopropoxide, etc. These all have different properties (solubility, thermal stability, etc.),

✉ Orsolya Kéri
keri.orsolya@mail.bme.hu

[1] Department of Inorganic and Analytical Chemistry, Budapest University of Technology and Economics, BudapestSzent Gellért tér 4, 1111, Hungary

[2] Department of Organic Chemistry and Technology, Budapest University of Technology and Economics, BudapestBudafoki út 8, 1111, Hungary

[3] Bulgarian Academy of Sciences, Georgi Nadjakov Institute of Solid State Physics, Tzarigradsko Chaussee 72, 1784 Sofia, Bulgaria

and consequently, choosing the precursor is based on what purpose the nanomaterial is prepared for. In many of the applications, the thermal stability of the sample is of great importance [23], and because of this, it has to be studied thoroughly.

In this work, polyvinylpyrrolidone/titanium tetraisopropoxide (PVP/TTIP) nanofibers were prepared from their alcoholic solution by electrospinning. Later from the PVP/TTIP composite, anatase and rutile TiO_2 nanofibers were prepared by annealing at different temperatures (550 °C and 900 °C, respectively) and in different atmospheres (oxidative and inert). The nanocomposite prepared by electrospinning and the different TiO_2 nanofibers were investigated by scanning electron microscopy (SEM), X-ray diffraction (XRD), and Raman spectroscopy.

To prepare oxide nanofibers from the electrospun fibers and also to be able to control the crystallinity and composition of the fibers, it was important to study the thermal properties of the PVP/TTIP fibers thoroughly. The thermal properties of the composite were investigated in air and nitrogen atmospheres by simultaneous thermogravimetry/differential thermal analysis (TG/DTA). The evolved gases were analyzed by on-line coupled mass spectrometry (TG/DTA-MS) [24–26], which was previously not done in the literature when these precursors were used for the preparation of TiO_2 nanofibers [27].

Experimental

Electrospinning was done using a homemade setup. For the preparation of the PVP/TTIP composite fibers, 1 g of titanium tetraisopropoxide (TTIP, $Ti(OiPr)_4$ by Sigma-Aldrich) was dissolved in the mixture of 1 cm^3 of acetic acid (AcOH) and 1 cm^3 of ethanol (EtOH). The solution was stirred for 15 min at room temperature. After this, 0.5 g of polyvinylpyrrolidone [PVP, $(C_6H_9NO)_n$, K-90 by Merck] was separately dissolved in 3 cm^3 of ethanol. The two solutions were then mixed together and stirred for 1 h at room temperature before the electrospinning [28]. The electrospinning was done at 25 kV voltage, the characteristic distance was approximately 25 cm, and a feeding rate of 4 cm^3 h^{-1} was used. The fibers were collected on an Al foil screen covered by a polyethylene sheet.

After the preparation of the composite nanofibers, the thermal properties were investigated. The measurements were carried out in an SDT 2960 Simultaneous DTA/TGA (TA Instruments Inc.) thermal analyzer. The samples were heated up to 900 °C using a heating rate of 10 °C min^{-1} in air and inert (nitrogen) atmospheres as well. Evolved gases were measured by a ThermoStar GSD 200 (Balzers Instruments) quadrupole mass spectrometer (MS) in multiple ion detection (MID) mode. The selected m/z ions could be measured in 64 channels simultaneously. A heated (200 °C) 100% methyl deactivated fused silica capillary provided the on-line coupling.

Based on the TG results, the PVP/TTIP fibers were later annealed at different temperatures in order to produce both anatase and rutile TiO_2 nanofibers. The temperatures were chosen based on the known phase transformations of TiO_2. Except for extremely small particles, at atmospheric pressure, the anatase-to-rutile transition is around 600 °C [29]. Thus, for preparing anatase TiO_2 fibers, the composite was heated up to 550 °C by which temperature the polymer completely burned out. Rutile TiO_2 nanofibers were achieved by annealing at 900 °C. The annealing was carried out in both air and nitrogen. In all cases, the heating rate was 10 °C min^{-1}.

The morphology of all samples was studied by scanning electron microscopy (SEM) in a JEOL JSM-5500LV scanning electron microscope. The measurements were done at 20 kV voltage. Before the measurement, the nanofibers were coated with a thin Au/Pd layer in a sputter coater.

The XRD patterns were recorded by a PANalytical X'pert Pro MPD X-ray diffractometer using Cu K_α irradiation.

Raman spectra were measured by a LabRam system (Horiba Jobin–Yvon, Lyon, France) coupled with an external 532 nm Nd-YAG laser source (Sacher Lasertechnik, Marburg, Germany).

Results and discussion

Based on the SEM pictures, the as-prepared PVP/TTIP fibers (Fig. 1a) were fairly uniform and had a diameter of about 800–900 nm. No bead formation could be observed.

The thermal analysis of these fibers was done in both oxidative (air) and inert atmospheres (N_2).

On the TG curve in nitrogen atmosphere (Fig. 2) till 100 °C, there was just a small mass loss ($\sim$ 6%), which could be assigned as the loss of physically adsorbed water and a very small amount of solvent that was used during the electrospinning. After this, on the TG curve, only one larger step could be seen between 250 °C and 600 °C, which was endothermic. At 250 °C, based on the MS spectra, just the TTIP started to decompose, which can be proved by the appearance of the methyl (m/z = 15) and the isopropoxide (m/z = 59) fragments (Table 1). Then, from around 280–300 °C, the PVP begun to decompose as well (a PVP fragment at m/z = 84 and the PVP monomer at m/z = 111 appeared on the MS spectra). In nitrogen, the decomposition of the PVP extremely stretched out and the organic compounds could not burn out totally. Caused by

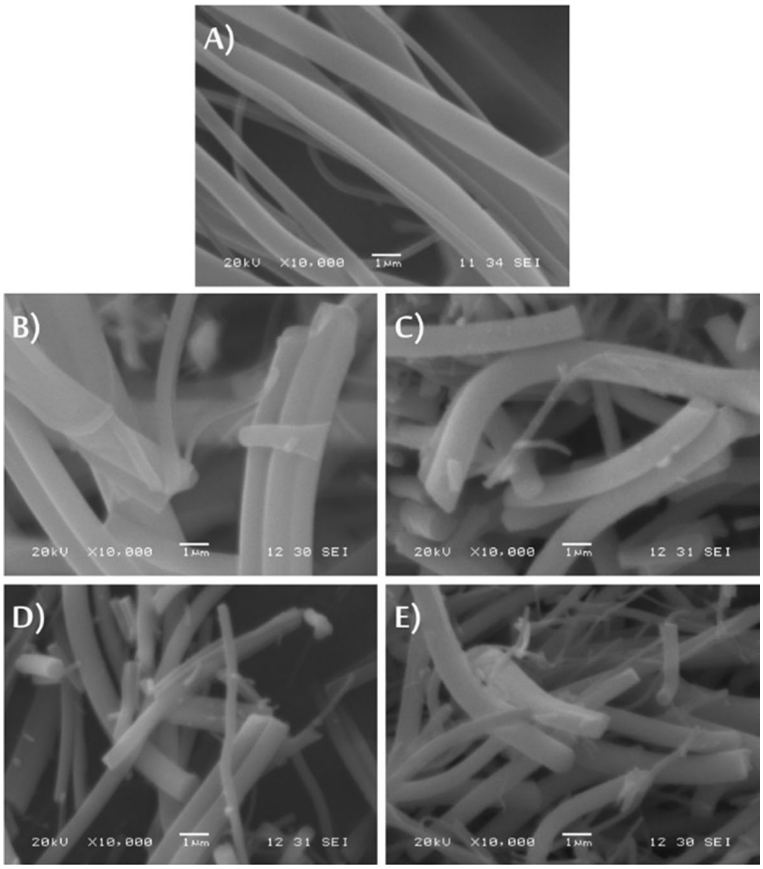

Fig. 1 SEM images of **a** PVP/TTIP fibers; **b** fibers annealed at 550 °C in N_2; **c** fibers annealed at 900 °C in N_2; **d** fibers annealed at 550 °C in air; **e** fibers annealed at 900 °C in air

this, the final product with a remaining mass of ~ 30% also contained some carbon residue beside TiO_2.

In air (Fig. 3), the decomposition started similarly with a mass loss of about 6% of water by 100 °C. The intense decomposition of the sample started at around 250 °C and consisted of two exothermic steps. Taking into account the MS results as well, it was obvious that the degradation again started with the TTIP (appearance of the fragment $m/z = 59$) (Table 1). In air, the organic material started to burn, and the endothermic heat of decomposition was overcompensated by the exothermic combustion heat, leading to exothermic DTA peaks. At around 350 °C, the decomposition was so rapid that the generated heat led to the excision of the temperature set by the heating program. This was indicated by the retraction of all the TG, DTG, and DTA curves. The degradation of the PVP also started later in air than that of the TTIP, and at first, the polymer chains of the PVP broke up and the side chains were severed, so only the organic backbone of the polymer remained, which was the last to decompose. The whole process was followed by the evolution of CO_2 as well. In air, by 350 °C, the TTIP decomposed totally, and by 550 °C, all the organic char residues from the PVP burnt out completely. The remaining mass was around 24%, and the final product only contained TiO_2. This was later confirmed by the XRD measurements.

On the SEM pictures after the annealing (Fig. 1b–e), it was visible that in all the cases the fibrous structure was maintained, but the fibers broke into shorter pieces. The diameter slightly decreased after the annealing in N_2 (700–800 nm), and the shrinking of the fibers was more significant when air was used as atmosphere (600–700 nm).

On the XRD diffractograms (Fig. 4), it could be seen that the electrospun PVP/TTIP fibers were amorphous. After annealing either in air or in nitrogen at 550 °C, only peaks referring to TiO_2 could be found, the nanofibers contained mostly anatase TiO_2 (ICDD 01-083-2243). A small peak at 27° appeared as well, indicating the presence of a smaller amount of rutile phase beside anatase. The chosen temperature was close to the phase transition temperature, so the appearance of this peak could be explained by that the formation of the rutile phase has already begun in a small part of the samples. When the annealing temperature was higher (900 °C), the fibers crystallized mostly in rutile form (ICDD 00-021-1276); however, a part of the sample was still anatase, based on the peaks.

The Raman spectra (Fig. 5) were in agreement with the XRD results. At 900 °C, the peaks of rutile TiO_2 can be

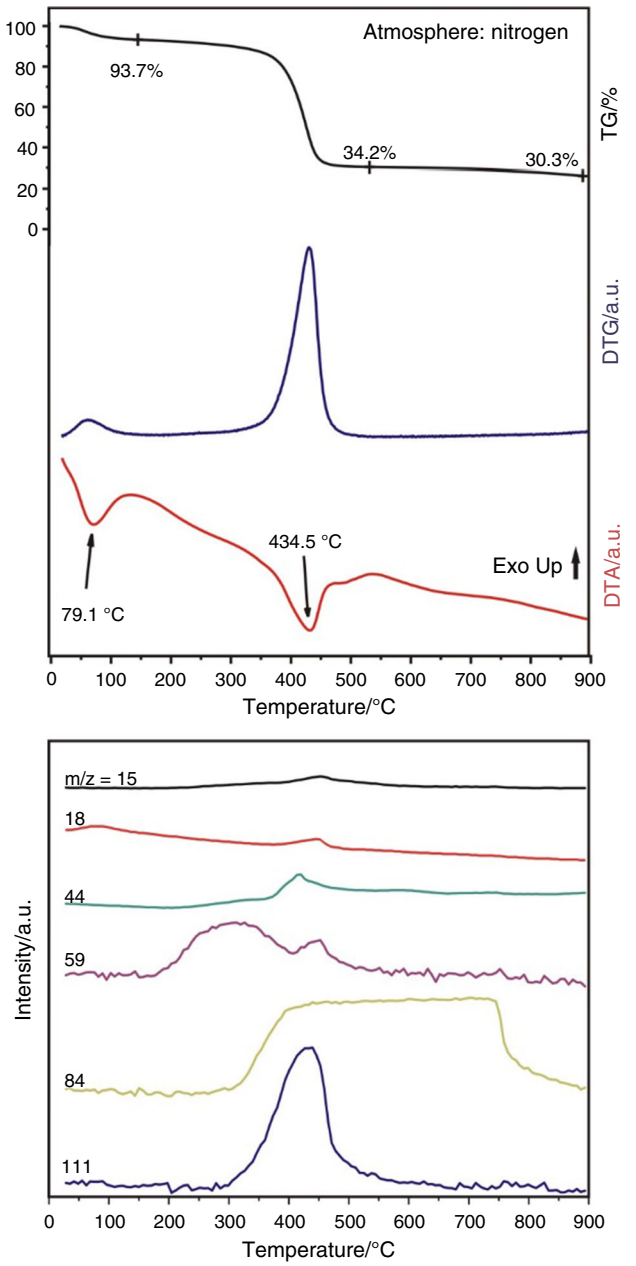

Fig. 2 Thermal analysis of the PVP/TTIP composite fibers in nitrogen

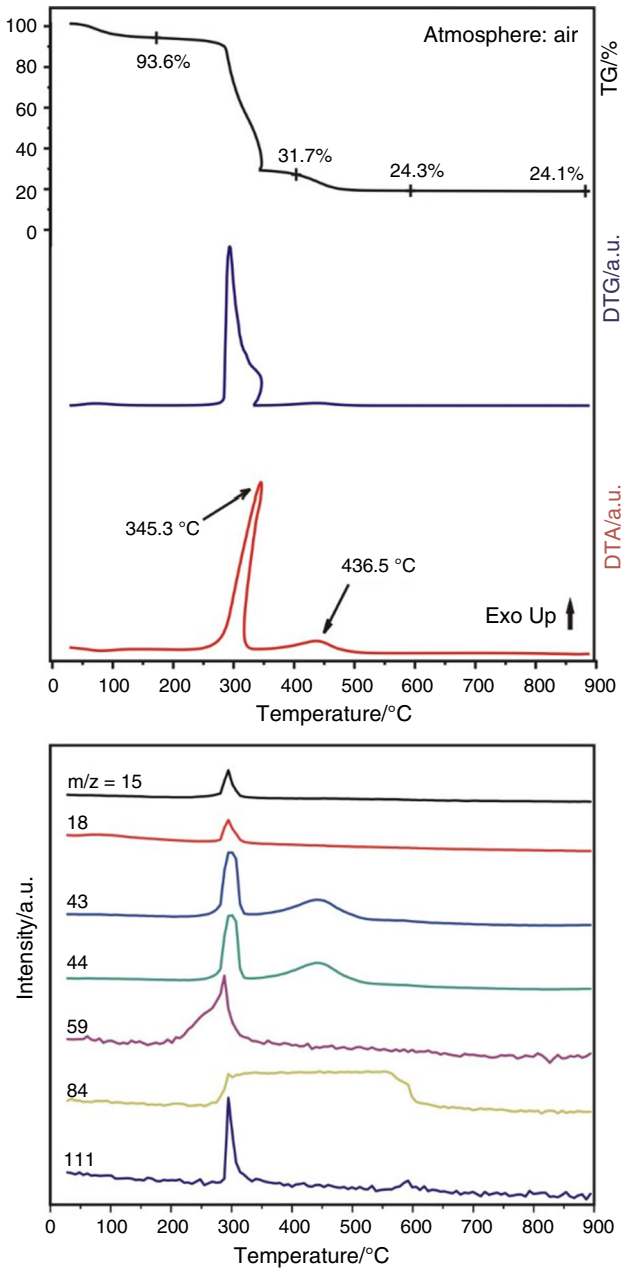

Fig. 3 Thermal analysis of the PVP/TTIP composite fibers in air

seen on the spectra (the peaks at around 243 cm^{-1}, 447 cm^{-1}, and 612 cm^{-1} can be, respectively, assigned to the second-order Raman scattering, E_g and A_{1g} modes of rutile TiO_2 [28, 30]), and also some small peaks of the anatase remained. However, at 550 °C, only the anatase TiO_2 peaks were visible. (The peaks at 144 cm^{-1}, 403 cm^{-1}, 520 cm^{-1}, 639 cm^{-1} are the E_g, B_{1g}, A_{1g} or B_{2g}, and E_g modes of the anatase phase [8, 31], respectively.) The Raman studies also confirmed that in nitrogen as expected from the TG/DTA-MS results some carbon residue remained (D and G bands of carbon appeared [32, 33]),

Table 1 Fragments of the materials in TG/DTA-MS measurement

m/z	Fragment	Molecular formula	Origin
15	CH_3	CH_3	TTIP
18	H_2O	H_2O	PVP, TTIP
43	CH_3–CH–CH_3	C_3H_7	TTIP
44	CO_2	CO_2	PVP, TTIP
59	Isopropoxide	C_3H_7O	TTIP
84	PVP fragment	C_4H_6NO	PVP
111	PVP monomer	C_6H_9NO	PVP

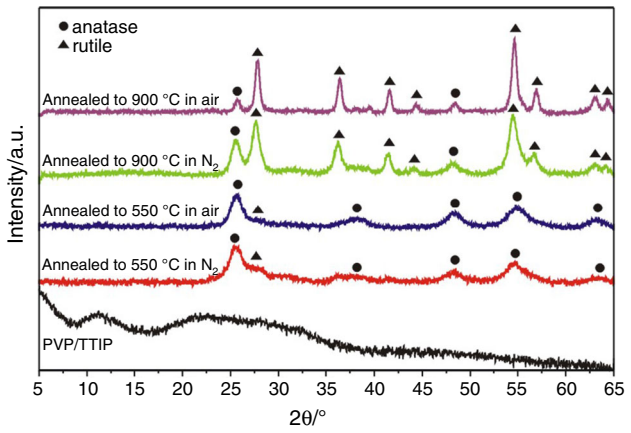

Fig. 4 XRD results of the PVP/TTIP and annealed fibers

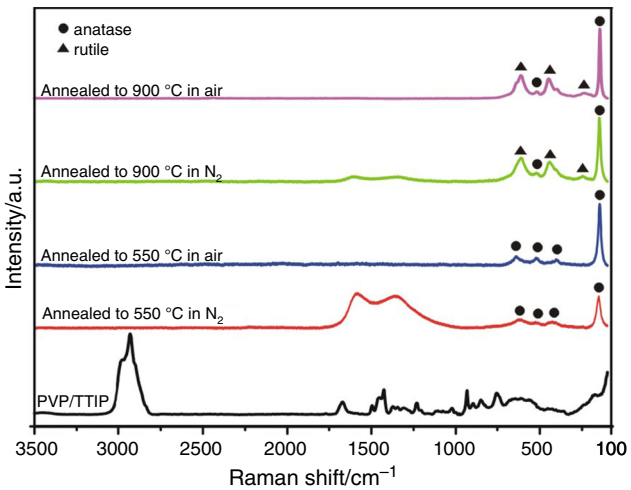

Fig. 5 Raman measurement of the PVP/TTIP and annealed fibers

while in air the polymer was burnt completely, and only the peak of crystalline TiO_2 appeared.

Conclusions

Polyvinylpyrrolidone/titanium tetraisopropoxide (PVP/TTIP) nanofibers with a diameter of 800–900 nm were prepared by electrospinning. The thermal properties of these fibers were thoroughly studied by TG/DTA, and the steps of decomposition were explained based on the results and the evolved gas analysis; the latter was previously not measured for these materials, when they were used for electrospinning. To be able to control the crystallinity and composition of the fibers, when later they were annealed to prepare TiO_2 nanofibers, studying the thermal properties was also important. For annealing, two different temperatures (550 °C and 900 °C) were chosen and also two different atmospheres were used. At 550 °C anatase and at 900 °C, rutile TiO_2 fibers could be prepared. When the annealing was done in nitrogen, besides the oxide, the fibers contained a small amount of carbon as well. Controlling the carbon content could be useful in the future, if the fibers are used as photocatalyst [28], because the light absorption could be shifted to the visible range if the sample also contains a small amount of carbon in it.

Acknowledgements Open access funding provided by Budapest University of Technology and Economics (BME). I. M. Szilágyi thanks for a János Bolyai Research Fellowship of the Hungarian Academy of Sciences and an ÚNKP-18-4-BME-238 New National Excellence Program of the Ministry of Human Capacities, Hungary. A GINOP-2.2.1-15-2017-00084, an NRDI K 124212, and an NRDI TNN_16 123631 Grant are acknowledged. The research within project No. VEKOP-2.3.2-16-2017-00013 was supported by the European Union and the State of Hungary, co-financed by the European Regional Development Fund. The research reported in this paper was supported by the Higher Education Excellence Program of the Ministry of Human Capacities in the frame of Nanotechnology and Materials Science research area of Budapest University of Technology (BME FIKP-NAT).

Compliance with ethical standards

Conflict of interest The authors declare that they have no conflict of interest.

References

1. Gleiter H. Nanostructured materials: basic concepts and microstructure. Acta Mater. 2000;48:1–29.
2. Dhand C, Dwivedi N, Loh J, Jie N. Methods and strategies for the synthesis of diverse nanoparticles and their applications. RSC Adv. 2015;5:105003–37. https://doi.org/10.1039/C5RA19388E.
3. Mussa Farkhani S, Valizadeh A. Electrospinning and electrospun nanofibres. IET Nanobiotechnol. 2014;8:83–92. https://doi.org/10.1049/iet-nbt.2012.0040.
4. Thenmozhi S, Dharmaraj N, Kadirvelu K, Kim HY. Electrospun nanofibers: new generation materials for advanced applications. Mater Sci Eng B Solid-State Mater Adv Technol. 2017;217:36–48. https://doi.org/10.1016/j.mseb.2017.01.001.
5. Szilágyi IM, Nagy D. Review on one-dimensional nanostructures prepared by electrospinning and atomic layer deposition. J Phys: Conf Ser. 2014;559:1–13.
6. Kéri O, Kocsis E, Nagy ZK, Parditka B, Erdélyi Z, Szilágyi IM. Preparation of Al_2O_3 coated PVA and PVP nanofibers and Al_2O_3 nanotubes by electrospinning and atomic layer deposition. Rev Roum Chim. 2018;63:401–6.
7. Kadam VV, Wang L, Padhye R. Electrospun nanofibre materials to filter air pollutants: a review. J Ind Text. 2018;47:2253–80.
8. Szilágyi IM, Santala E, Heikkilä M, Pore V, Kemell M, Nikitin T, et al. Photocatalytic properties of WO_3/TiO_2 core/shell nanofibers

prepared by electrospinning and atomic layer deposition. Chem Vap Depos. 2013;19:149–55. https://doi.org/10.1002/cvde.201207037.
9. Malwal D, Gopinath P. Fabrication and applications of ceramic nanofibers in water remediation: a review. Crit Rev Environ Sci Technol. 2016;46:500–34.
10. Leng JY, Xu XJ, Lv N, Fan HT, Zhang T. Synthesis and gas-sensing characteristics of WO_3 nanofibers via electrospinning. J Colloid Interface Sci. 2011;356:54–7. https://doi.org/10.1016/j.jcis.2010.11.079.
11. Abideen ZU, Kim J-H, Lee J-H, Kim J-Y, Mirzaei A, Kim HW, et al. Electrospun metal oxide composite nanofibers gas sensors: a review. J Korean Ceram Soc. 2017;54:366–79. http://www.jkcs.or.kr/journal/view.php?number=8066.
12. Ke H. Morphology and thermal performance of quaternary fatty acid eutectics/polyurethane/Ag form-stable phase change composite fibrous membranes. J Therm Anal Calorim. 2017;129:1533–45.
13. Choi SJ, Persano L, Camposeo A, Jang JS, Koo WT, Kim SJ, et al. Electrospun nanostructures for high performance chemiresistive and optical sensors. Macromol Mater Eng. 2017;302:1–37.
14. Wen P, Zong MH, Linhardt RJ, Feng K, Wu H. Electrospinning: a novel nano-encapsulation approach for bioactive compounds. Trends Food Sci Technol. 2017;70:56–68. https://doi.org/10.1016/j.tifs.2017.10.009.
15. Patil JV, Mali SS, Kamble AS, Hong CK, Kim JH, Patil PS. Electrospinning: a versatile technique for making of 1D growth of nanostructured nanofibers and its applications: an experimental approach. Appl Surf Sci. 2017;423:641–74. https://doi.org/10.1016/j.apsusc.2017.06.116.
16. Sabzehmeidani MM, Karimi H, Ghaedi M. Electrospinning preparation of NiO/ZnO composite nanofibers for photodegradation of binary mixture of rhodamine B and methylene blue in aqueous solution: central composite optimization. Appl Organomet Chem. 2018;32:1–15.
17. Pal B, Bakr ZH, Krishnan SG, Yusoff MM, Jose R. Large scale synthesis of 3D nanoflowers of SnO_2/TiO_2 composite via electrospinning with synergistic properties. Mater Lett. 2018;225:117–21. https://doi.org/10.1016/j.matlet.2018.04.120.
18. Yang CM, Kim BH. Highly conductive pitch-based carbon nanofiber/MnO_2 composites for high-capacitance supercapacitors. J Alloys Compd. 2018;749:441–7. https://doi.org/10.1016/j.jallcom.2018.03.305.
19. Kim ID, Rothschild A. Nanostructured metal oxide gas sensors prepared by electrospinning. Polym Adv Technol. 2011;22:318–25.
20. Kim J, Lee J, Kim J, Kim SS. Synthesis of aligned TiO_2 nanofibers using electrospinning. Appl Sci. 2018;8:309. http://www.mdpi.com/2076-3417/8/2/309.
21. Massaglia G, Quaglio M. Semiconducting nanofibers in photoelectrochemistry. Mater Sci Semicond Process. 2018;73:13–21.
22. Mondal K, Sharma A. Recent advances in electrospun metal-oxide nanofiber based interfaces for electrochemical biosensing. RSC Adv. 2016;6:94595–616.
23. Szilágyi IM, Santala E, Kemell M, Nikitin T, Khriachtchev L, Räsänen M, et al. Thermal study on electrospun polyvinylpyrrolidone/ammonium metatungstate nanofibers: optimising the annealing conditions for obtaining WO_3 nanofibers. J Therm Anal Calorim. 2011;105:73–81.
24. Stanciu I, Predoana L, Pandele Cusu J, Preda S, Anastasescu M, Vojisavljević K, et al. Thermal behaviour of the TiO_2-based gels obtained by microwave-assisted sol–gel method. J Therm Anal Calorim. 2017;130:639–51.
25. Santhana Krishnan G, Murali N, Jafar Ahamed A. Structural transformation, thermal endurance, and identification of evolved gases during heat treatment processes of carbon fiber polymer precursors focusing on the stereoregularity. J Therm Anal Calorim. 2017;129:821–32.
26. Justh N, Berke B, László K, Szilágyi IM. Thermal analysis of the improved Hummers' synthesis of graphene oxide. J Therm Anal Calorim. 2018;131:2267–72.
27. Cacciotti I, Bianco A, Pezzotti G, Gusmano G. Synthesis, thermal behaviour and luminescence properties of rare earth-doped titania nanofibers. Chem Eng J. 2011;166:751–64. https://doi.org/10.1016/j.cej.2010.07.008.
28. Boyadjiev SI, Kéri O, Bárdos P, Firkala T, Gáber F, Nagy ZK, et al. TiO_2/ZnO and ZnO/TiO_2 core/shell nanofibers prepared by electrospinning and atomic layer deposition for photocatalysis and gas sensing. Appl Surf Sci. 2017;424:190–7. https://doi.org/10.1016/j.apsusc.2017.03.030.
29. Hanaor DAH, Sorrell CC. Review of the anatase to rutile phase transformation. J Mater Sci. 2011;46:855–74.
30. Meng F, Liu Y, Xue T, Su Q, Wang W, Qi T. Structures, formation mechanisms, and ion-exchange properties of α-, β-, and γ-Na_2TiO_3. RSC Adv. 2016;6:112625–33. http://xlink.rsc.org/?DOI=C6RA16984H.
31. Potlog T, Dobromir M, Luca D, Onufrijevs P, Medvids A, Shamardin A. Rutile to anatase phase transition in TiO_2:Nb thin films by annealing in H2 atmosphere. Curr Appl Phys. 2016;16:826–9.
32. Saito R, Hofmann M, Dresselhaus G, Jorio A, Dresselhaus MS. Raman spectroscopy of graphene and carbon nanotubes. Adv Phys. 2011;60:413–550.
33. Nanda SS, Kim MJ, Yeom KS, An SSA, Ju H, Yi DK. Raman spectrum of graphene with its versatile future perspectives. Trends Analyt Chem. 2016;80:125–31. https://doi.org/10.1016/j.trac.2016.02.024.